Supplement of Biogeosciences, 16, 3267–3282, 2019
https://doi.org/10.5194/bg-16-3267-2019-supplement

Biogeosciences Open Access EGU

Supplement of

Temporal variability in foraminiferal morphology and geochemistry at the West Antarctic Peninsula: a sediment trap study

Anna Mikis et al.

Correspondence to: Katharine R. Hendry (k.hendry@bristol.ac.uk)

1. Weekly averages of sediment trap data

All foraminifera specimens were removed from the sediment trap cups, and counted. The data presented in the main text represent number of specimens per m^2 per day, averaged to a one day period. To account for the production and settling time the flux records were shifted by one week based on Nps sinking speeds of 0.189 to 0.431 cm/s reported by Von Gyldenfeldt et al. (2000). The time-shifted Nps flux and stable isotope records were used to create average annual composite figures (Figures S1 and S2) following methods used by Jonkers et al. (2010).

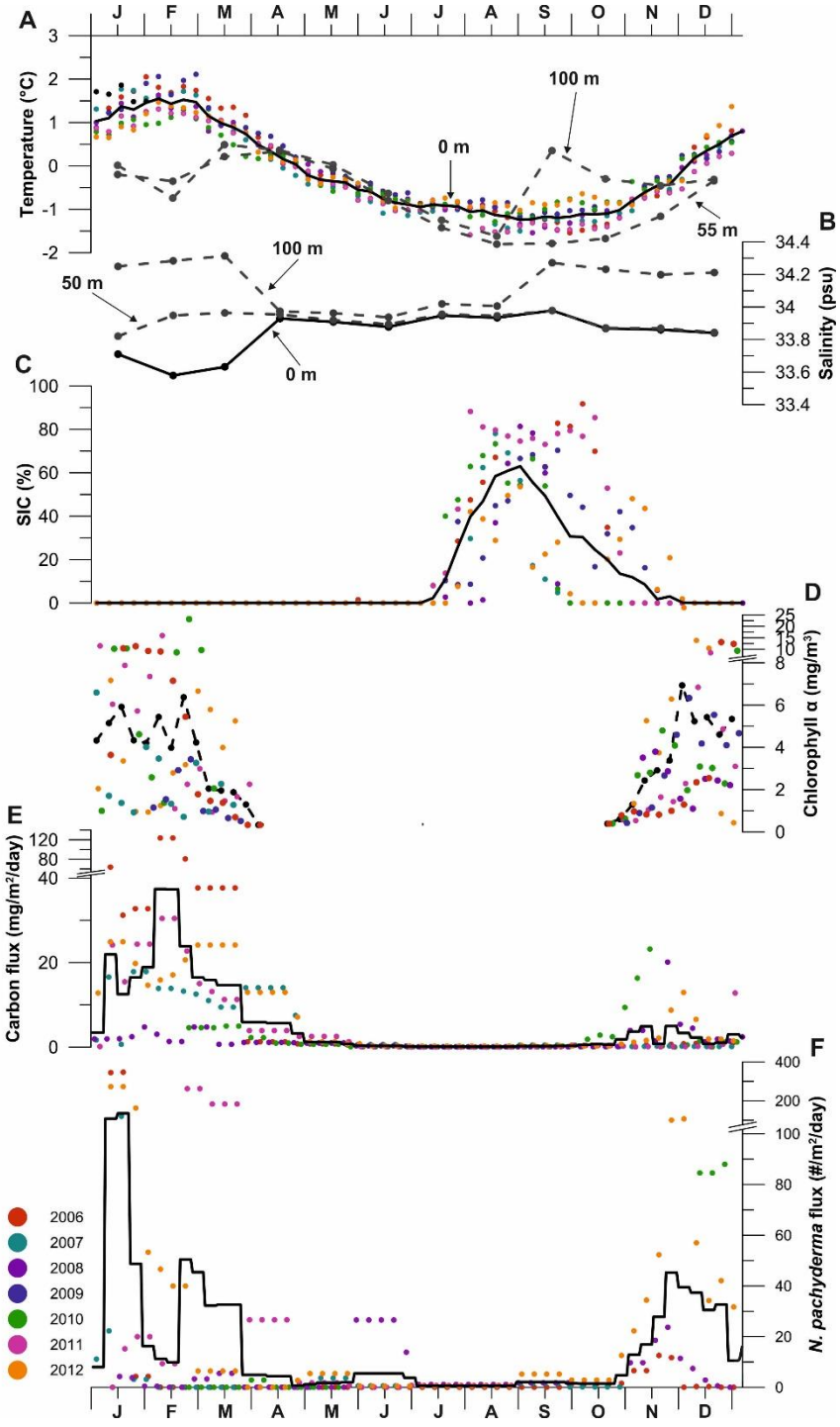

Figure S1: Weekly averaged and time-shifted time series flux record (solid lines: average values of 2006-2012 period; coloured dots are individual years). A) Annual satellite-derived weekly SST (black line) and WOA13 monthly temperature at 55 m and 100 m water depths (grey lines). B) WO13 monthly salinity record at surface (black line), 50 and 100 m (grey lines). C) Annual satellite-derived daily sea-ice concentration. D) Average chlorophyll *a* concentration (10-20m), E) Average organic carbon flux. F) Nps flux record (extremely high flux of 2010 removed from calculation). The low fluxes of early January and sudden drop-off at the end of December are due to gaps in the sampling period.

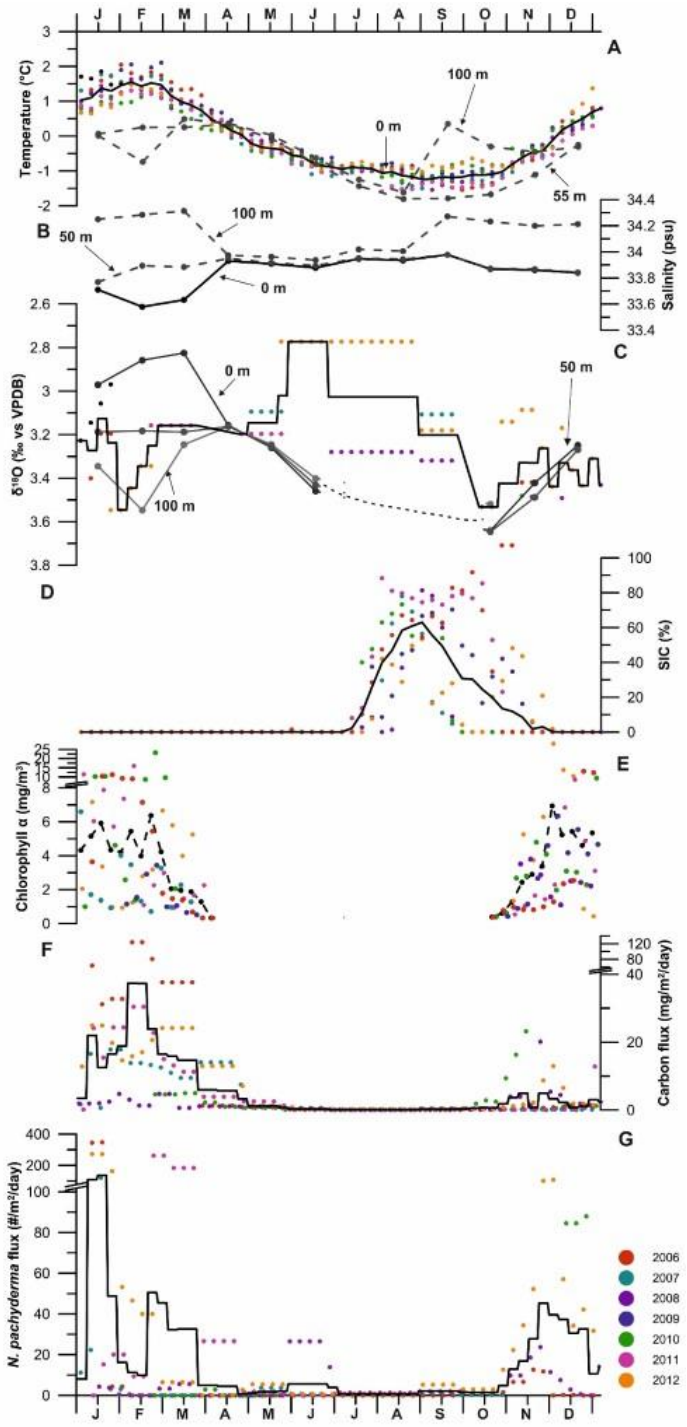

Figure S2: Weekly averaged and time-shifted time series □$^{18}O_{np}$ record (solid lines: average values of 2006-2012 period; coloured dots are individual years). A) Annual satellite-derived weekly SST (black line) and WOA13 monthly temperature at 55 m and 100 m water depths (grey lines). B) WO13 monthly salinity record at surface (black line), 50 and 100 m (grey lines). C) Multi-specimen $\delta^{18}O^{np}$ record, $\delta^{18}O_{eq}$ at surface, 50 and 100 m water depths. D) Annual satellite-derived daily sea-ice concentration. E) Average chlorophyll *a* concentration (10-20 m), F) Average organic carbon flux. G) Nps flux record (extremely high flux of 2010 removed from calculation).

Table S1: Nps flux statistics summary

Mean	286.76
Median	3.68
Standard deviation	1392.73
Variance	1939695.83
Minimum	0
Maximum	9586.29
Mean + 1σ	1679.49
Mean + 2σ	3072.22
Quartile 1	0
Quartile 2	3.68
Quartile 3	23.7
Top outliers (Q3+(1.5xIQR))	>59.3

2. Anderson-Darling tests for normality of morphometric data

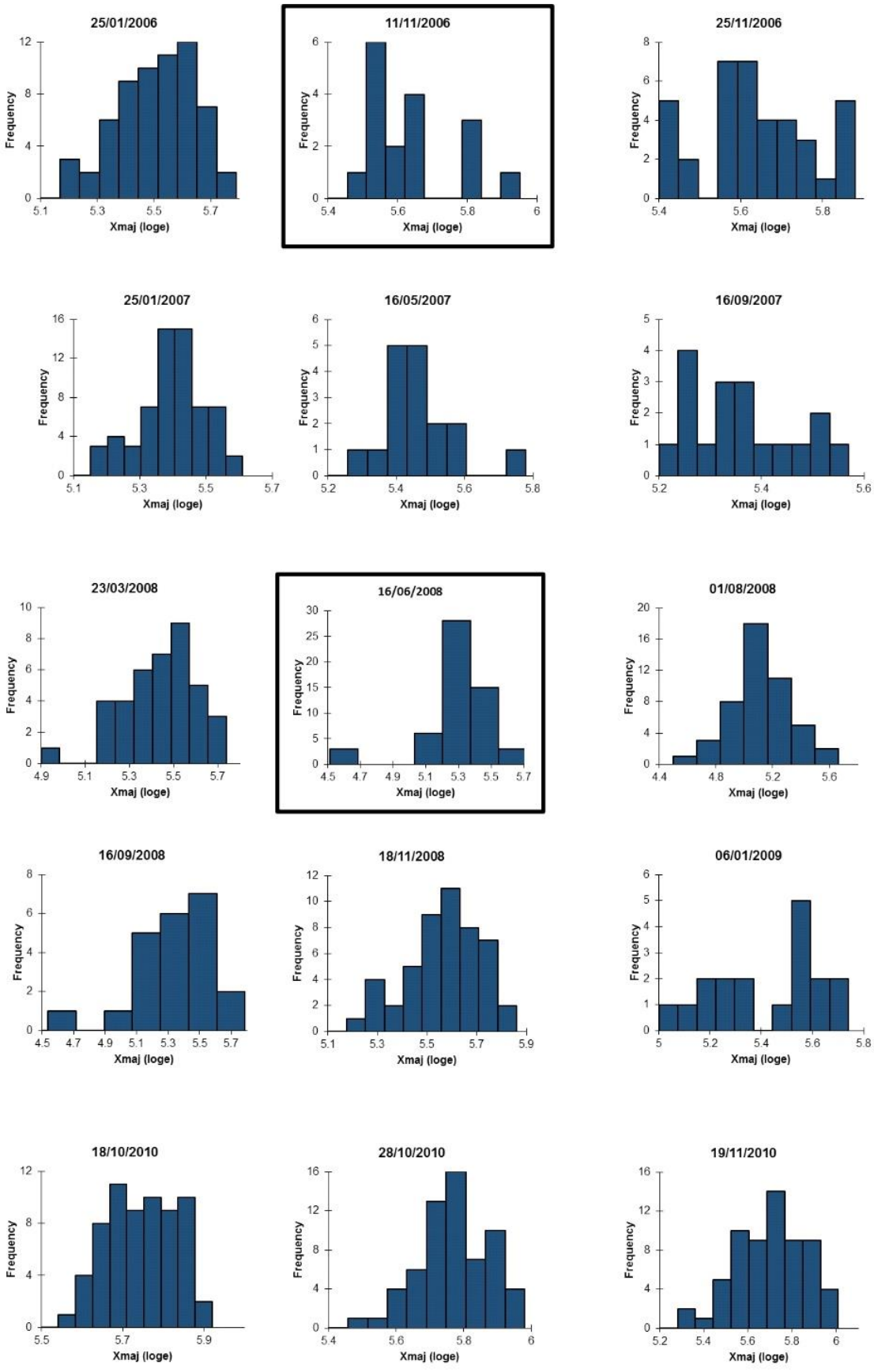

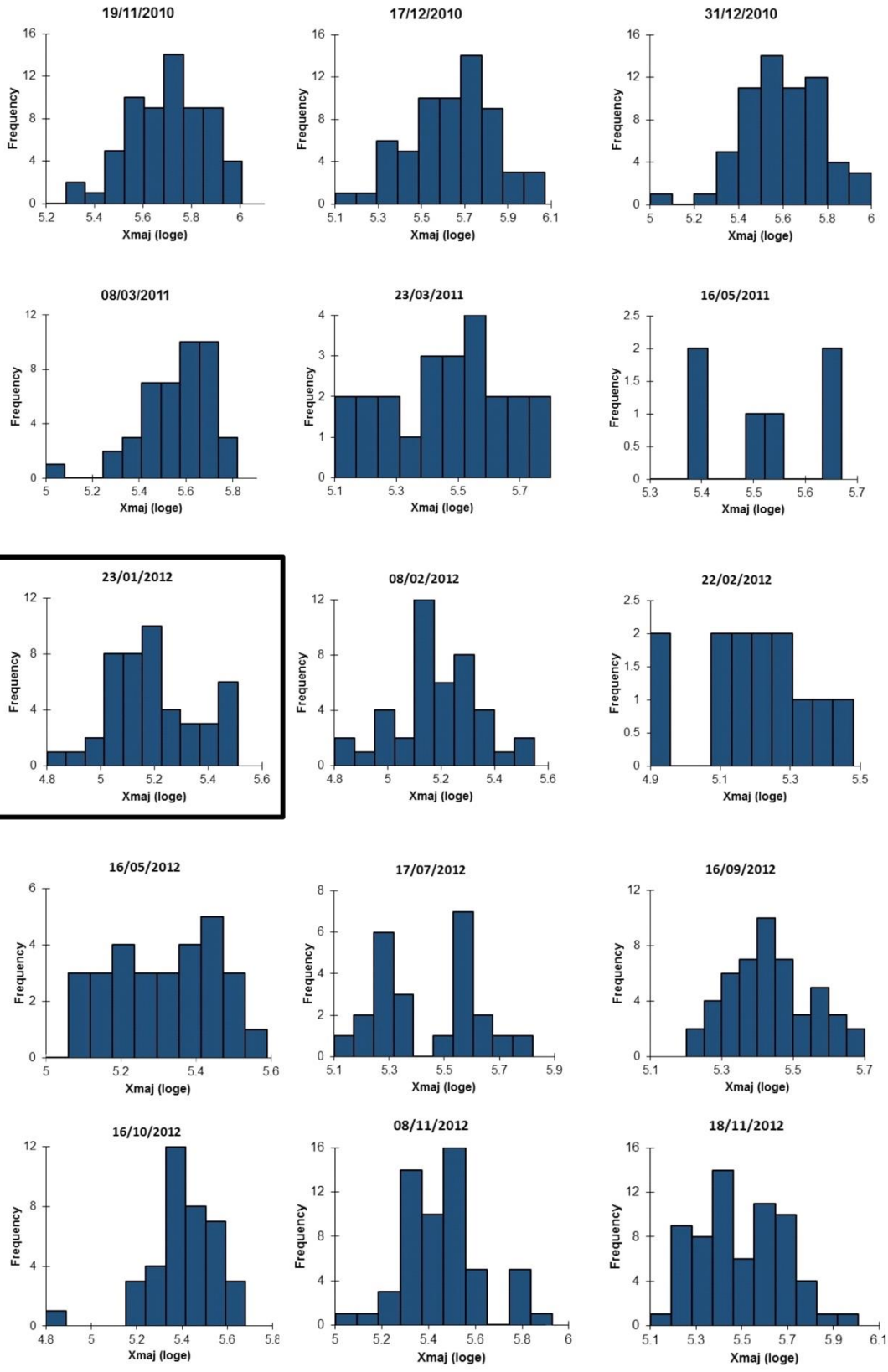
19/11/2010
17/12/2010
31/12/2010
08/03/2011
23/03/2011
16/05/2011
23/01/2012
08/02/2012
22/02/2012
16/05/2012
17/07/2012
16/09/2012
16/10/2012
08/11/2012
18/11/2012
Frequency
Xmaj (loge)

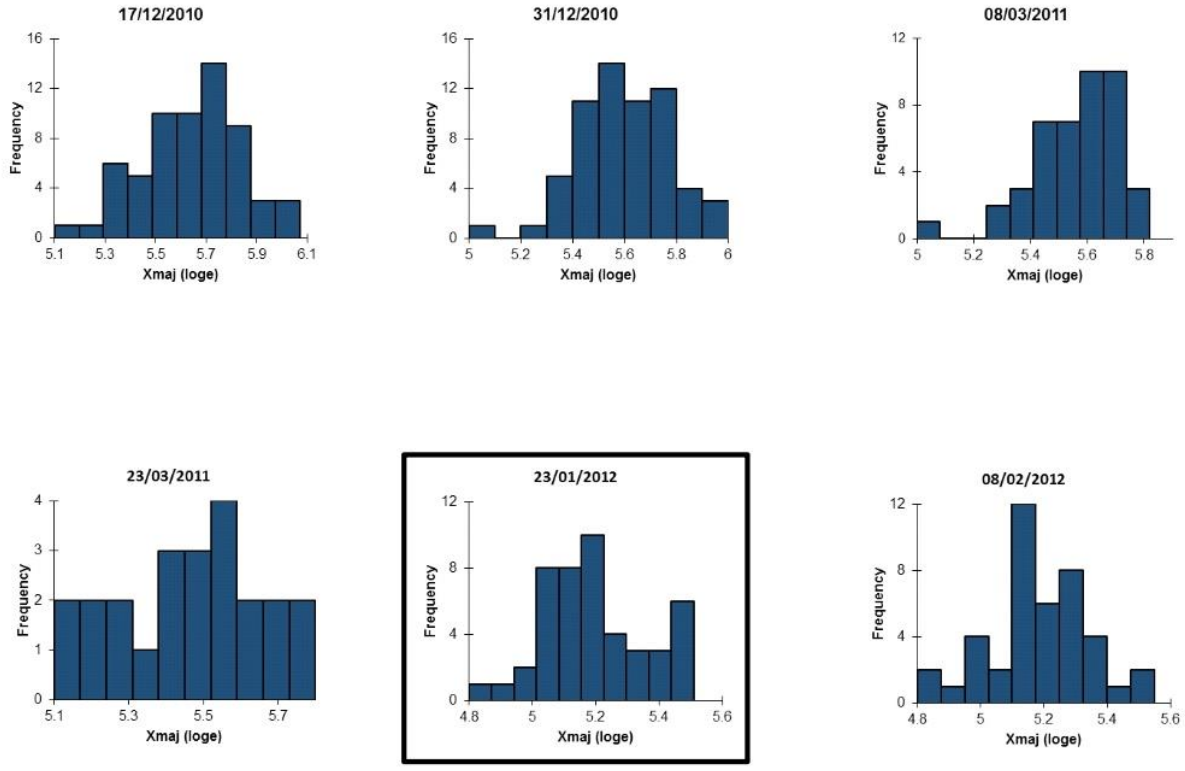

Figure S3: Histograms of the log-transformed maximum diameter values of each sample. Non-normally distributed datasets are highlighted with black outline (Anderson-Darling Normality test; $p<0.05$).

3. Results of Principal Component Analyses of morphometric data

The distributions of the four size-invariant morphological parameters (circularity ratio, box ratio, elongation ratio and compactness coefficient, Table S2), which relate to test shape, were analysed within each sample (manually collected dataset) using principal component analysis (PCA) (representative sample shown in main text). The presence of multiple clusters and thus multiple growth stages can also be supported by undertaking Anderson-Darling test for normality on the first principle component site scores. Fourteen of the 32 samples display a non-normal distribution (Table S3) indicating that in those 14 samples both pre-adult and adult specimens are likely present. To assess the relationship between the test size and the test shape the log-transformed maximum diameter of each specimen was plotted against the first principal component scores (for example, see main text). The two parameters correlated with each other in 12 of the 32 samples (Table S3) (four samples were discounted from the total of 36 samples due to the number of specimens being less than 15, see main text; Figure S4). The linear correlation coefficients (r values) were between −0.48 and 0.51, which suggests variable relationship between shape and size, i.e. positive correlation – as a specimen becomes larger it also becomes more rounded or in the case of negative correlations the specimens were more rounded the smaller they were. The result from the largest sample is shown in Figure S5.

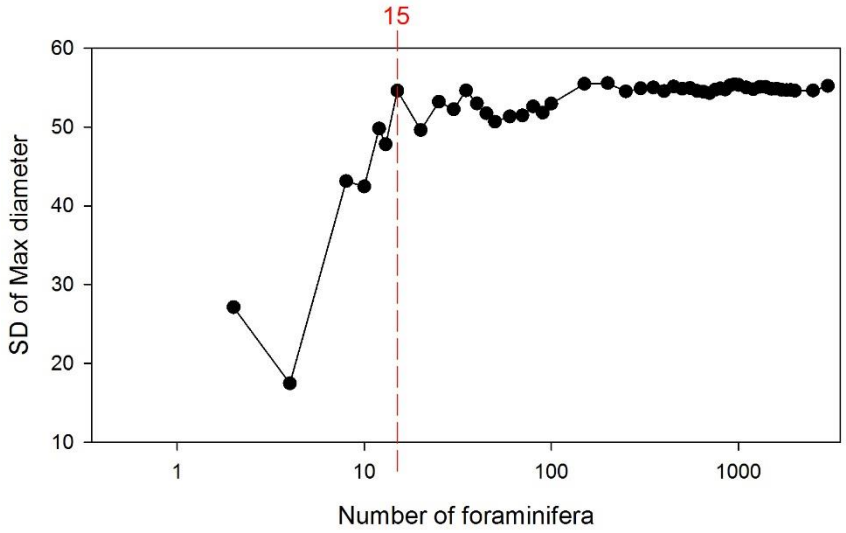

Figure S4: Rarefaction curve for maximum diameter, showing standard deviation of measurements versus foraminiferal count number.

Table S2: Definition of secondary morphological parameters, which relate to test shape as opposed to test size are derived from measured parameters (Moller et al. 2013).

Primary parameters		Secondary morphological parameters	
p	Perimeter	Rc = A*4*π / p2	Circularity ratio
A	Area	Re = 2*√A / (Xmax *√π)	Elongation ratio
Xmax	Maximum diameter	B = Xmin/Xmax	Box ratio
Xmin	Minimum diameter	C = p / 2*√π*√A	Compactness coefficient

Table S3: Mid-date of collection period for sediment trap samples, number of data points per sample, Anderson-Darling p value of significance of the 1st principal component scores (f1) of the PCA conducted on the normalised size-invariant morphological dataset, and the correlation coefficient, r, calculated between the log-transformed maximum diameter (Xmaj) and F1. Significant values are highlighted in bold.

Date	Count	Anderson-Darling p value	Xmaj(ln)-Size-invariant PCA F1 r value
25/01/2006	62	0.225	-0.118
11/11/2006	17	0.517	-0.110
25/11/2006	38	0.503	-0.213
25/01/2007	63	0.203	0.043
16/05/2007	17	0.308	-0.083
16/09/2007	18	**0.045**	-0.035
23/03/2008	39	0.358	-0.216
16/06/2008	55	**0.030**	**-0.338**
01/08/2008	48	**0.001**	**0.442**
16/09/2008	22	0.373	0.081
18/11/2008	49	0.390	0.037
06/01/2009	18	0.114	0.262
18/10/2010	64	0.527	**-0.480**
28/10/2010	63	**0.009**	**-0.324**
19/11/2010	63	**0.009**	**0.323**
17/12/2010	62	0.054	-0.025
31/12/2010	62	**0.029**	0.248
08/03/2011	43	**<0.0001**	0.124
23/03/2011	23	0.180	**0.508**
23/01/2012	46	**0.000**	0.046
08/02/2012	42	**0.016**	-0.214
16/05/2012	29	0.297	**0.480**
17/07/2012	24	**0.006**	0.136
16/09/2012	49	**0.000**	-0.033
16/10/2012	38	0.103	0.010
08/11/2012	56	0.051	**-0.291**
18/11/2012	65	**<0.0001**	**-0.431**
02/12/2012	64	0.151	**-0.351**
09/12/2012	50	0.539	**-0.353**
23/12/2012	50	0.051	-0.148
30/12/2012	64	**0.011**	-0.235
27/01/2013	61	**0.004**	**-0.389**

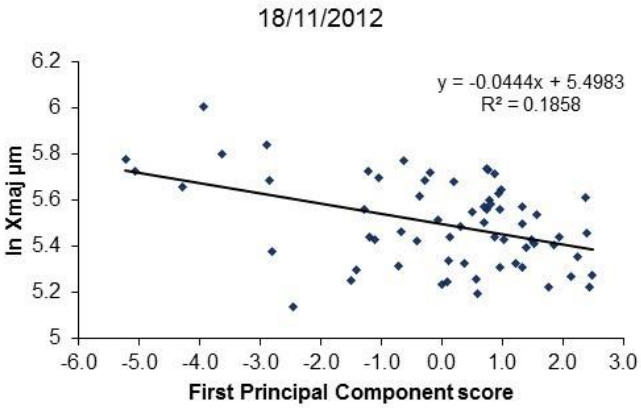

Figure S5: Relationship between the log-transformed maximum diameter (ln Xmaj) and the 1st principal component scores of the PCA conducted on the normalised size-invariant morphological values. Figure shown is from 18/11/2012, which contains the largest number of specimens analysed.

To assess the relationship between the shape and the size parameters in each set of samples, PCA was performed on the mean values of the log-transformed maximum diameter and the mean values of each size-invariant morphological parameter of the 36 sets of data (Figure S6, Table S4). Three principal components explain 99.9% of the variability in the dataset. The first principal component (F1) is strongly correlated with the size-invariant variables (Table S4). It increases with increasing circularity, elongation and box ratio and increases with decreasing compactness coefficient. This suggests that these four criteria covary. F1 can therefore be viewed as a measure of circularity ratio, elongation ratio, box ratio, and compactness coefficient. F1 correlates most strongly with elongation ratio and box ratio with correlation coefficients of 0.819 and 0.792 (Table S4) indicating that the first principal component is primarily a measure of these two variables and the observed variability in the dataset is related to changes in elongation in two dimensions, i.e. how elongate or round the specimens are, which relates to the ratio between the minor axis and major axis. The second principal component (F2) is also correlated with circularity ratio, elongation ratio, box ratio, and compactness coefficient, but to a lesser degree. Strongest correlation is recorded between circularity ratio and F2 (−0.641) (Table S4), so this component (F2) can be viewed as a measure of how close to a perfect sphere the specimens are. The third principal component (Figure S7 – F1-F3 biplot) only makes up 17% of the total variability in the dataset in comparison to the 49% and 33% of contribution of F1 and F2, respectively. However, it does show a strong positive correlation with maximum diameter (r = 0.840, Table S4 Xmaj) suggesting that this component is a measure of specimen size. The biplot of the PCA results reveal these strong correlations between the principal components and the variables. PCA biplots are used mainly to determine groupings of observations based on the positions of the variables with respect to the principle components. In Figure S7 the observations are scattered across both F1 and F2 and that observations which belong to the same seasons do not cluster together.

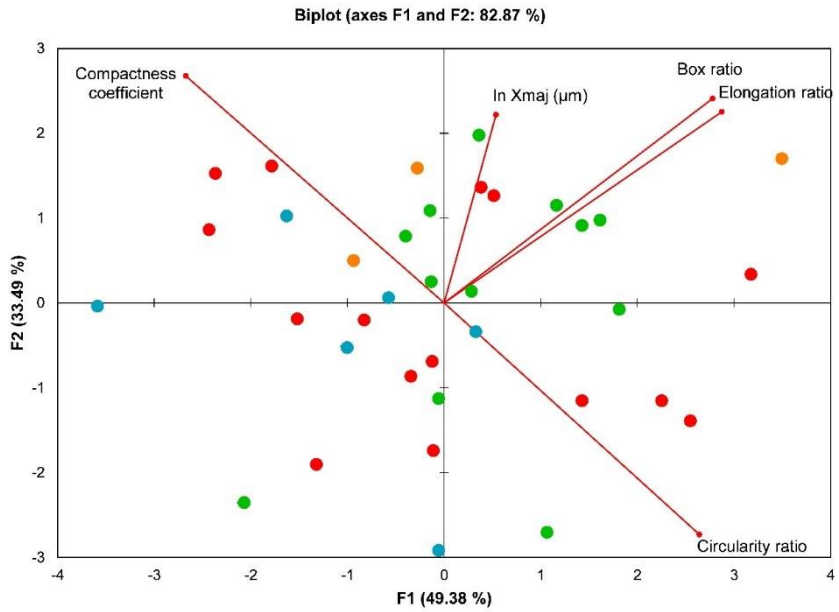

Figure S6: PCA biplot (F1-F2 scores) of the mean values of log-transformed maximum diameter and the mean values of each size-invariant morphological parameter covering the time series. Seasons are identified as: green = spring, red = summer, orange = autumn, and blue = winter.

The dataset used for the PCA analysis was separated out based on the presence/absence of correlation between log-transformed MD and first principal component scores of PCA on size-invariant

morphological parameters within a given sample. Two PCAs were carried out on the datasets separated by the presence/absence of correlation between log-transformed maximum diameter and F1 of the PCA conducted on the normalised size-invariant morphological dataset (Table S2). These showed similar results to the PCA that was carried out on the dataset which was not separated by the correlation (Figure S8, Table S4). Neither PCA show any clear clustering of points based on seasonal separation of the data (Figure S8). Differences arise when the impact of the morphological variables is considered on the principle components. In the dataset where no correlation exits between the log-transformed MD and the first principal component scores of PCA on size-invariant morphological parameters 99% of the variability can be explained by three principal components (Figure S8) which is similar to the results of the PCA analysis conducted on the entire dataset together (Figure S7). Correlation between the morphological variables and the principal components (Figure S8) is also similar to the relationships identified in the PCA of the data from the 32 sediment trap samples (Figure S7): F1 and F2 correlate strongly with size-invariant variables, F3 with log-transformed maximum diameter, but the directions of the correlations are the opposite. In Figure S7 (dataset where samples show no relationship between shape and size) F1 is most strongly correlated with compactness coefficient and circularity ratio ($r = 0.867$ and -0.864 respectively), suggesting that it is a measure of how compact and perfectly spherical a specimen is. F2 shows similarly strong correlations with elongation ratio and box ratio ($r= 0.817$ and 0.837), therefore we can consider F2 to be a measure of how elongated a specimen is in two dimensions (box ratio is equal to the ratio between minimum diameter and maximum diameter). In the dataset where samples show a significant relationship between shape and size the first two principal components can explain over 90% of the variability. Here F1 is strongly correlated with the size-invariant variables and F2 with the log-transformed maximum diameter (Figure S8). Similarly to the results of the PCA conducted on the entire dataset prior to splitting it up (Figure S6) F1 is most strongly correlated with elongation ratio and box ratio ($r=0.941$ and 0.939, respectively), therefore it can be considered to be a measure of these two variables. F2 is a measure of specimen size as it is only correlated with log-transformed maximum diameter ($r= 0.83$). Hence, based on these findings, the results of the PCA conducted on the original dataset of 36 observations is highly influenced by the samples where a statistically significant relationship exists between the log-transformed MD (indicative of specimen size) and the size-invariant morphological parameters (indicative of shape). The lack of clustering into groups in any of the PCA biplots indicates that the observed morphological variability is related to a combination of environmental parameters acting on the wellbeing of the foraminifera (see main text for discussion).

Table S4: Eigenvalues and correlation between variables and principal component factors of the PCA of the mean values of log-transformed maximum diameter and the mean values of each size invariant morphological parameters of the times series.

Eigenvalues			
	F1	F2	F3
Eigenvalue	2.469	1.675	0.852
Variability (%)	49.381	33.493	17.031
Cumulative %	49.381	82.874	99.905
Correlations between variables and factors			
	F1	F2	F3
Circularity ratio	0.753	-0.641	0.147
Elongation ratio	0.819	0.529	-0.220
Box ratio	0.792	0.565	-0.227
Compactness coefficient	-0.762	0.628	-0.157
ln Xmaj (µm)	0.153	0.521	0.840

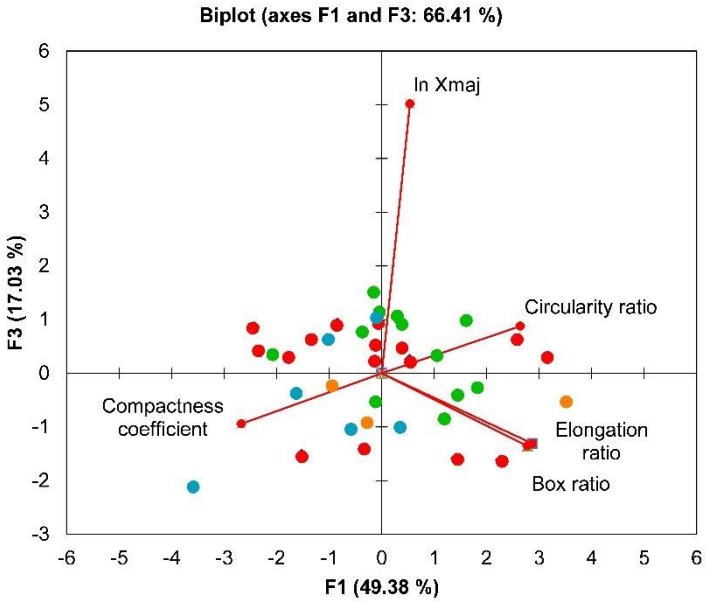

Figure S7: PCA biplot (F1-F3 scores) of the mean values of the log-transformed maximum diameter and the mean values of each size invariant morphological parameters covering the time series. Seasons are identified as: green = spring, red = summer, orange = autumn, and blue = winter.

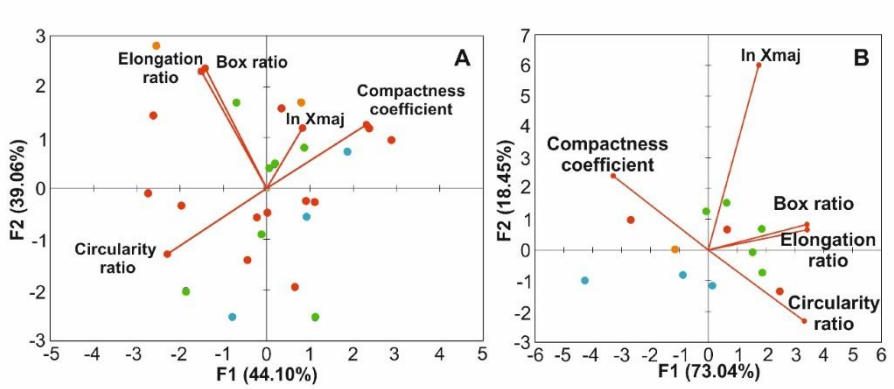

Figure S8: PCA biplots of the mean values of the log-transformed maximum diameter and the mean values of each size invariant morphological parameters belonging to samples where no correlation was found in Table S2.
Seasons are identified as: green = spring, red = summer, orange = autumn, and blue = winter.

To summarise the findings of this section:

- Statistical analysis supports the use of log-transformed maximum diameter as a measure of Nps size in a population (Figure S3).
- Inter-and intra-annual variability of Nps size is supported by statistical analysis.
- Specimens of different life stages are identified in 14 out of 32 samples by PCA.
- Positive and negative linear correlation between test shape and test size is found in 12 out of 32 samples.
- PCA revealed that size-invariant morphological parameters, particularly elongation and box ratio exert the greatest influence on test shape.
- The results of the PCA conducted on the entire dataset (36 samples) are strongly influenced by samples where statistically significant correlation exists between test shape and test size.
- The PCA analyses revealed no clustering of data points related to the seasons the samples derive from suggesting that the morphological variability is the result of a combination of variable environmental parameters (food availability, temperature, sea ice, etc).

4. Comparing automated and manual morphometric data

	Manual				Automated			
Date	Mean (μm)	Median (μm)	Var raw	Var norm	Mean (μm)	Median (μm)	Var raw	Var norm
25/01/2006	251.63	253.36	1152.93	0.05	242.85	238.05	1541.67	0.04
11/11/2006	290.64	272.57	1835.35	0.08	285.75	270.42	1805.99	0.09
25/11/2006	288.75	281.48	1515.67	0.07	286.58	285.37	2100.71	0.05
25/01/2007	223.92	225.61	489.66	0.06	224.95	224.05	964.89	0.03
16/05/2007	240.69	235.14	957.73	0.05	245.29	236.17	1714.28	0.06
16/09/2007	218.25	213.40	599.00	0.08	221.13	218.19	612.34	0.08
23/03/2008	239.07	243.71	1636.13	0.05	245.37	248.06	1564.34	0.07
16/06/2008	208.47	211.41	1240.61	0.04	219.94	219.05	508.88	0.03
01/08/2008	171.43	163.96	1362.80	0.04	191.84	173.30	2194.57	0.09
16/09/2008	216.13	224.63	2221.53	0.06	219.01	221.72	1252.07	0.08
18/11/2008	269.11	269.59	1590.50	0.06	267.17	269.08	2121.51	0.06
09/12/2008	279.05	289.86	2283.97	0.10	254.59	253.51	2787.79	0.09
06/01/2009	236.89	249.42	2304.50	0.09	241.45	242.84	2236.07	0.11
18/10/2010	321.23	320.59	742.37	0.06	324.87	323.30	762.93	0.05
28/10/2010	325.30	330.48	2304.83	0.02	331.74	330.23	1067.02	0.05
19/11/2010	311.54	315.42	2412.81	0.05	300.04	302.07	2862.93	0.03
17/12/2010	292.87	293.88	3399.50	0.05	292.19	293.84	3424.12	0.03
31/12/2010	278.19	275.30	2598.75	0.04	306.81	304.27	2979.67	0.05
08/03/2011	268.92	274.49	1433.41	0.04	279.68	291.78	2385.11	0.05
23/03/2011	244.94	242.41	2253.77	0.08	244.75	241.80	2272.19	0.05
16/05/2012	209.99	211.63	943.57	0.07	200.13	209.25	1043.83	0.07
17/07/2012	237.31	233.02	1908.04	0.07	211.63	200.34	1637.21	0.09
16/09/2012	236.63	232.94	778.09	0.06	235.02	230.11	921.67	0.04
08/11/2012	243.38	241.30	2012.95	0.04	250.25	247.47	2139.62	0.04
18/11/2012	254.27	242.52	2376.29	0.04	265.64	255.16	2948.18	0.04
02/12/2012	279.29	280.43	4263.58	0.02	281.13	270.95	3841.31	0.03
09/12/2012	289.16	296.09	4267.76	0.05	244.23	241.77	1101.26	0.07
23/12/2012	278.20	264.38	3363.44	0.07	253.77	241.88	2968.27	0.06
30/12/2012	281.02	284.35	3872.97	0.05	275.53	271.03	2643.69	0.04
27/01/2013	257.70	262.00	1821.63	0.06	254.90	256.43	2575.27	0.03

Table S5 (over page): Comparison of the sample mean, medians, and variances (σ^2) of raw and normalised maximum diameter dataset measured by the manual and automated method. By normalising the maximum diameter (X_{max}) values ($X_{max,n} = (n - n_{min}) / (n_{max} - n_{min})$ it is possible to reduce the large range in the between sample variance (Moller et al., 2013).

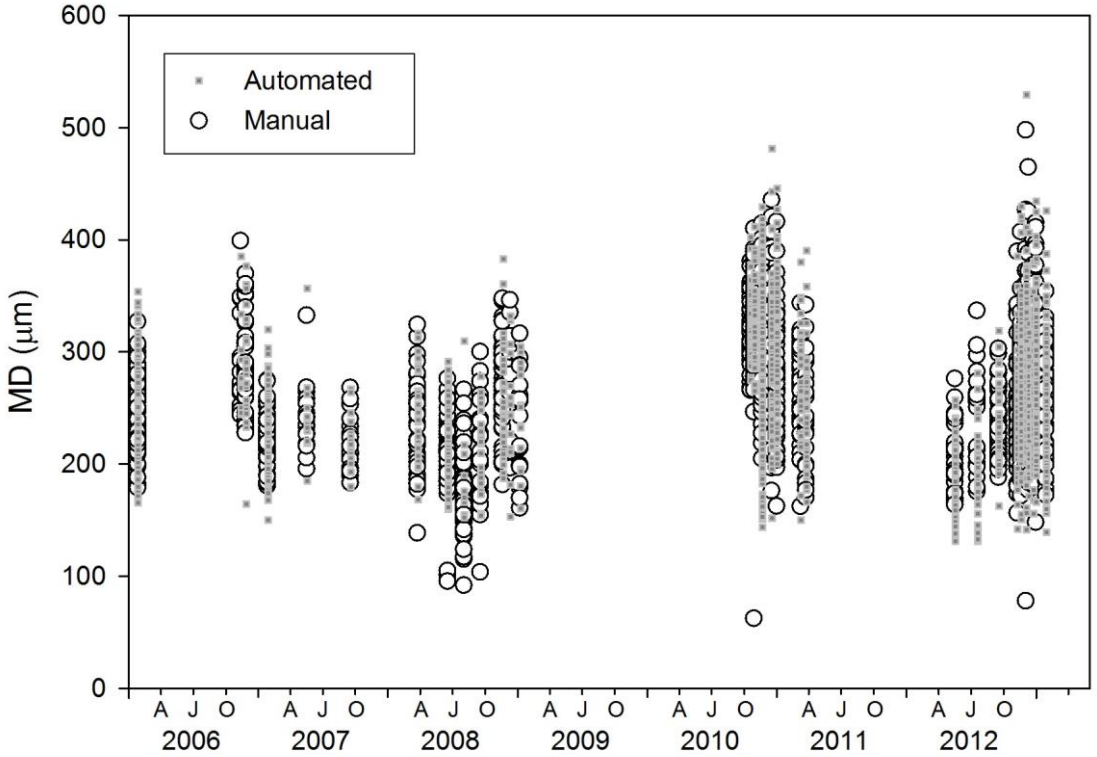

Figure S9: Plot of all automated and manual data collected from sediment trap foraminifera. AJO: April (autumn), July (winter), October (spring).

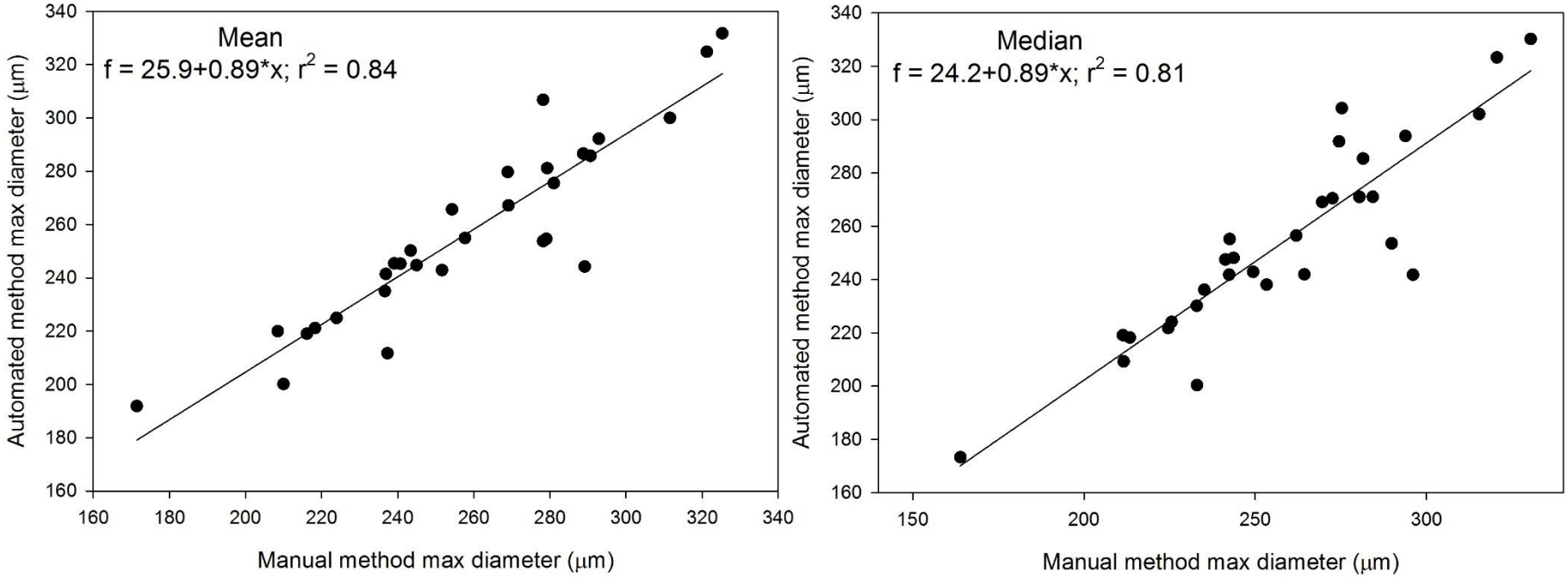

Figure S10: Correlation between the two methods, comparing (left) means of maximum diameters from each method and (right) medians. Linear regression equations and r^2 values given in each case.

Table S6: Results of Mann-Whitney U-tests (p values) and number of data points. Statistically significant (p<0.05) results are highlighted in bold

Date	p	n (Manual)	n (Automated)
25/01/2006	**0.048**	**62**	**435**
11/11/2006	0.851	17	11
25/11/2006	0.922	38	28
25/01/2007	0.914	63	129
16/05/2007	0.740	17	12
16/09/2007	0.704	18	15
23/03/2008	0.530	39	35
16/06/2008	**0.016**	**55**	**313**
01/08/2008	0.141	48	10
16/09/2008	0.974	22	24
18/11/2008	0.793	49	36
09/12/2008	0.191	12	17
06/01/2009	0.864	18	14
18/10/2010	0.557	64	62
28/10/2010	0.663	63	57
19/11/2010	0.162	63	471
17/12/2010	0.894	62	96
31/12/2010	**0.001**	**62**	**103**
08/03/2011	0.169	43	38
23/03/2011	0.917	23	48
16/05/2012	0.347	29	23
17/07/2012	0.122	24	11
16/09/2012	0.716	49	52
08/11/2012	0.246	56	59
18/11/2012	0.192	65	110
02/12/2012	0.903	64	108
09/12/2012	**<0.001**	**50**	**35**
23/12/2012	**0.028**	**50**	**59**
30/12/2012	0.482	64	136
27/01/2013	0.576	61	155

Table S7: **Correlation (r) and slope of regression values between maximum diameter and surface area measurements (manual data collection method) 32 samples of the time series (four samples with less than 15 specimens/sample were removed, see main text). Number of specimens in each sample and the r value at 95% statistical significance are also included in table.**

Date	*Correlation*	*r value at 0.05 significance*	*Count*	*Slope of regression*
25/01/2006	0.980	0.250	62	0.804
11/11/2006	0.969	0.456	17	0.855
25/11/2006	0.982	0.304	38	0.819
25/01/2007	0.969	0.250	63	0.852
16/05/2007	0.968	0.456	17	0.877
16/09/2007	0.959	0.444	18	0.816
23/03/2008	0.988	0.304	39	0.86
16/06/2008	0.987	0.273	55	0.791
01/08/2008	0.988	0.288	48	0.868
16/09/2008	0.994	0.400	22	0.833
18/11/2008	0.977	0.273	49	0.833
06/01/2009	0.991	0.444	18	0.85
18/10/2010	0.981	0.250	64	0.803
28/10/2010	0.992	0.250	63	0.822
19/11/2010	0.983	0.250	63	0.903
17/12/2010	0.983	0.250	62	0.836
31/12/2010	0.982	0.250	62	0.866
08/03/2011	0.983	0.288	43	0.888
23/03/2011	0.995	0.400	23	0.904
23/01/2012	0.990	0.288	46	0.826
08/02/2012	0.983	0.304	42	0.807
16/05/2012	0.976	0.349	29	0.915
17/07/2012	0.990	0.381	24	0.828
16/09/2012	0.968	0.273	49	0.852
16/10/2012	0.980	0.304	38	0.863
08/11/2012	0.979	0.250	56	0.778
18/11/2012	0.985	0.250	65	0.76
02/12/2012	0.984	0.250	64	0.772
09/12/2012	0.986	0.273	50	0.78
23/12/2012	0.985	0.273	50	0.807
30/12/2012	0.989	0.250	64	0.819
27/01/2013	0.974	0.250	61	0.766

Table S8: Spearman's correlation coefficient (r) values. Statistically significant ($p<0.05$) results are highlighted in bold. See cross-plots in figure S9.

Variable	**Nps flux**	**Carbon flux**	**Nitrogen flux**	**Sea-Ice Conc.**	**SST**	**Chlorophyll *a* conc.**
Nps flux	**1**	**0.229**	**0.219**	-0.035	0.112	-0.005
Carbon flux	**0.229**	**1**	**0.989**	**-0.493**	**0.790**	**0.312**
Nitrogen flux	**0.219**	**0.989**	**1**	**-0.480**	**0.770**	**0.309**
Sea Ice Conc.	-0.035	**-0.493**	**-0.480**	**1**	**-0.610**	0.160
SST	0.112	**0.790**	**0.770**	**-0.610**	**1**	0.077
Chlorophyll a conc.	-0.005	**0.312**	**0.309**	0.160	0.077	**1**

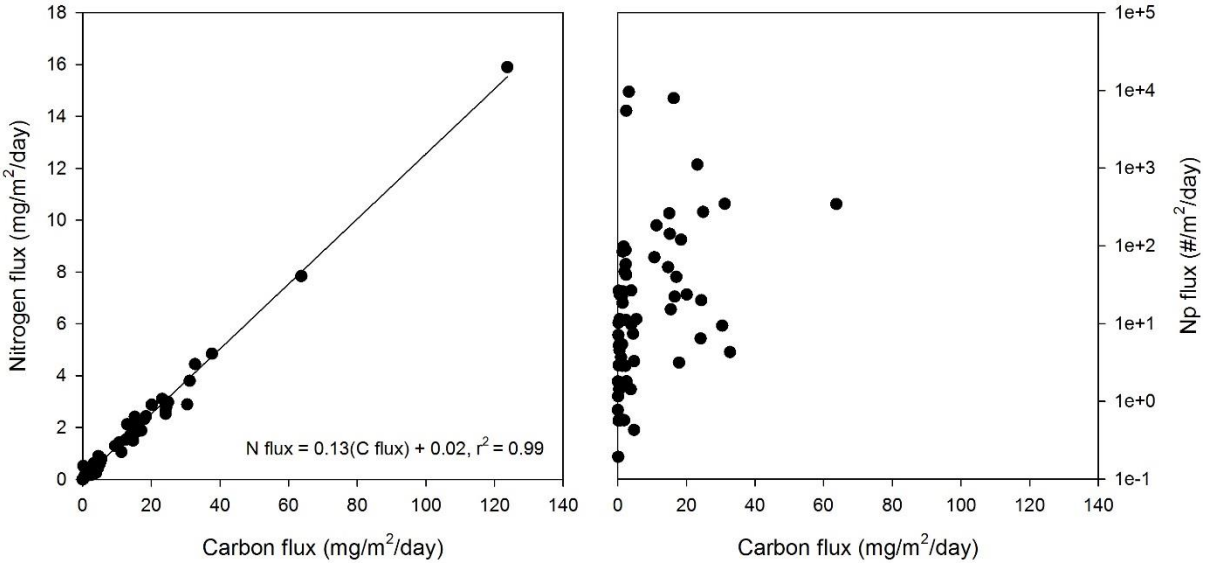

Figure S11: Cross-plots of carbon flux in sediment traps and (left) nitrogen flux and (right) foraminiferal flux.

5. Relative frequency plots of stable isotope data

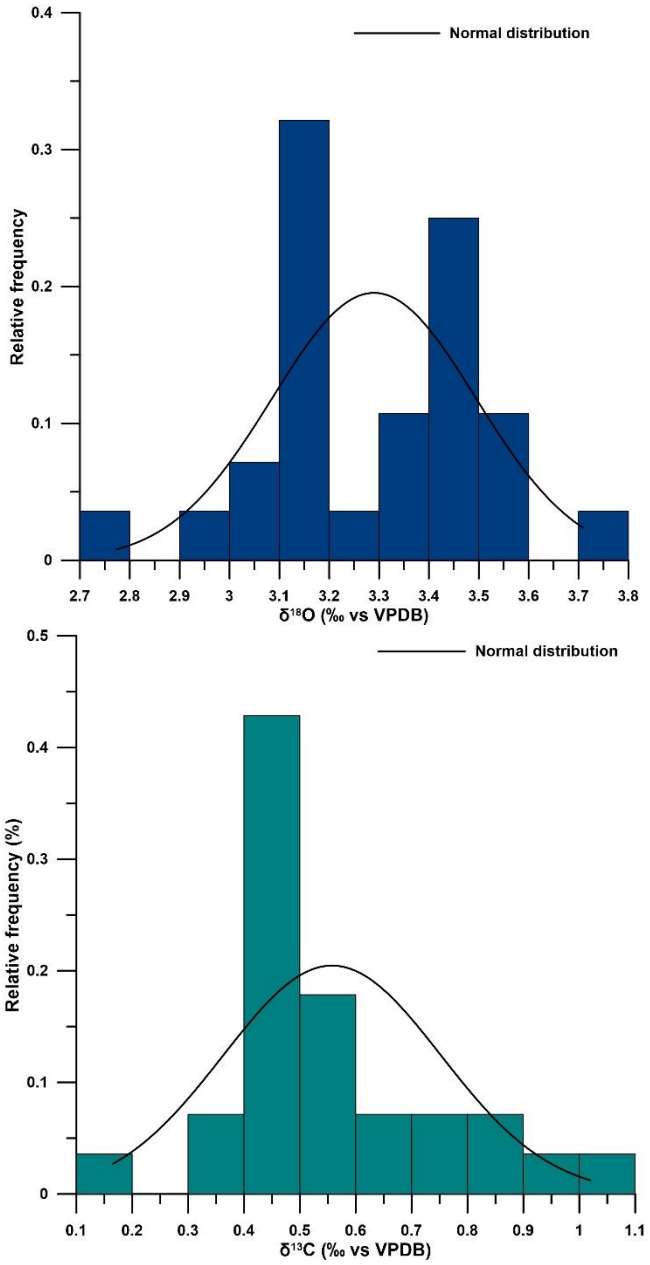

Figure S12: Relative frequency histogram of bulk (top) $\delta^{18}O_{np}$ and (bottom) $\delta^{13}C_{np}$. Black line represents the expected normal distribution. Anderson-Darling test for normality (results as p values) revealed a normal distribution for $\delta^{18}O_{np}$ and non-normal distribution for $\delta^{13}C_{np}$.

6. Calculated seawater oxygen isotope profiles

To compensate for the lack of year-round $\delta^{18}O_{sw}$ data WOA13 salinity (Zweng et al., 2013) data were used to calculate expected $\delta^{18}O_{sw}$ values for the period between January and October using Equation A:

$$\delta^{18}O_{sw} = 0.3387 \times S - 11.796 \quad (A)$$

where S is salinity (Meredith et al., 2017). An alternative $\delta^{18}O_{sw}$ equation (Equation B) was used to calculate $\delta^{18}O_{sw}$ for the period between October and December due to the introduction of glacial and sea ice melt into the surface water during the spring. Only surface values (0-50 m) were calculated for the October-December period as only surface water (0-50 m) $\delta^{18}O_{sw}$ measurements exist for this period.

$$\delta^{18}O_{sw} = 0.0458 \times S - 1.8883 \quad (B)$$

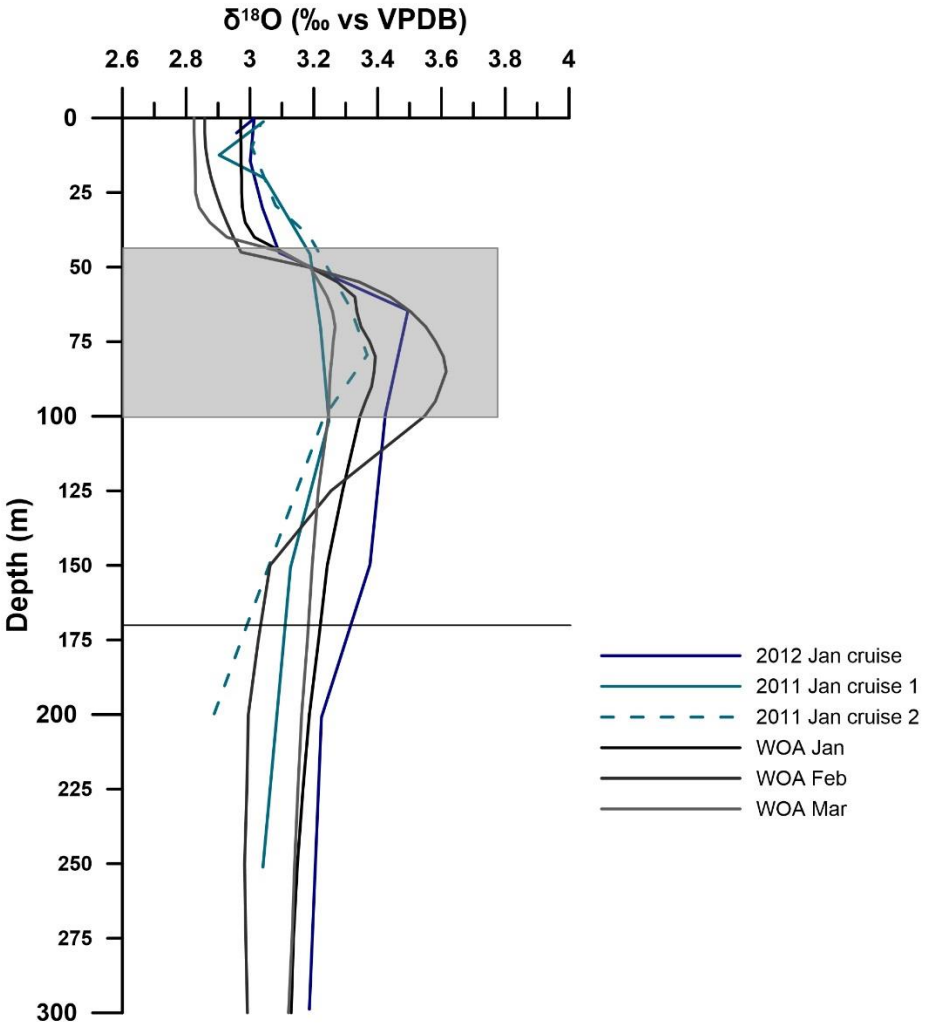

Figure S13: $\delta^{18}O_{eq}$ depth profiles calculated from direct $\delta^{18}O_{sw}$ observations from Meredith et al. (2016; blue) and from calculated $\delta^{18}O_{sw}$ data based on WOA13 salinity measurements (grey). Grey box shows our calculated depth range of Nps.

7. Link between stable isotopic composition and size in *N. pachyderma*

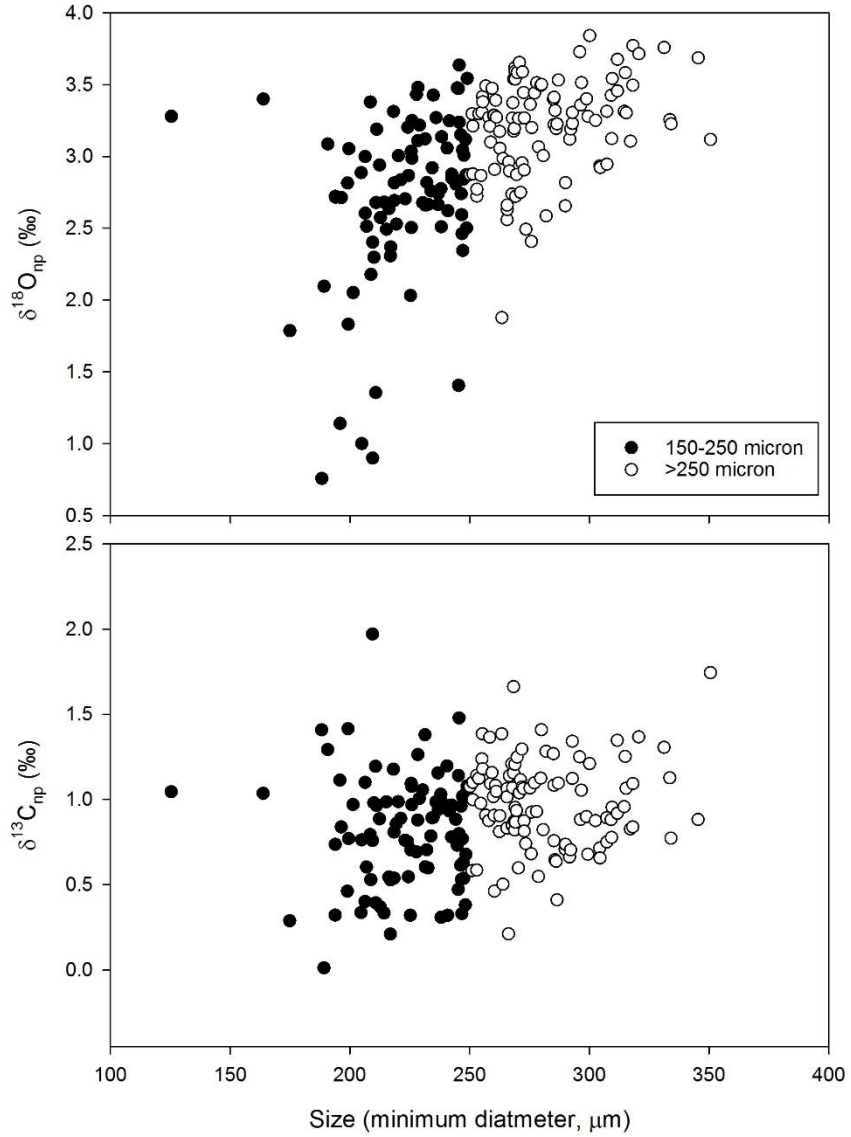

Figure S14: Cross plots of *N. pachyderma* shell size (minimum diameter) and isotopic composition. See main text for correlation statistics.

7. Sea-ice dynamics

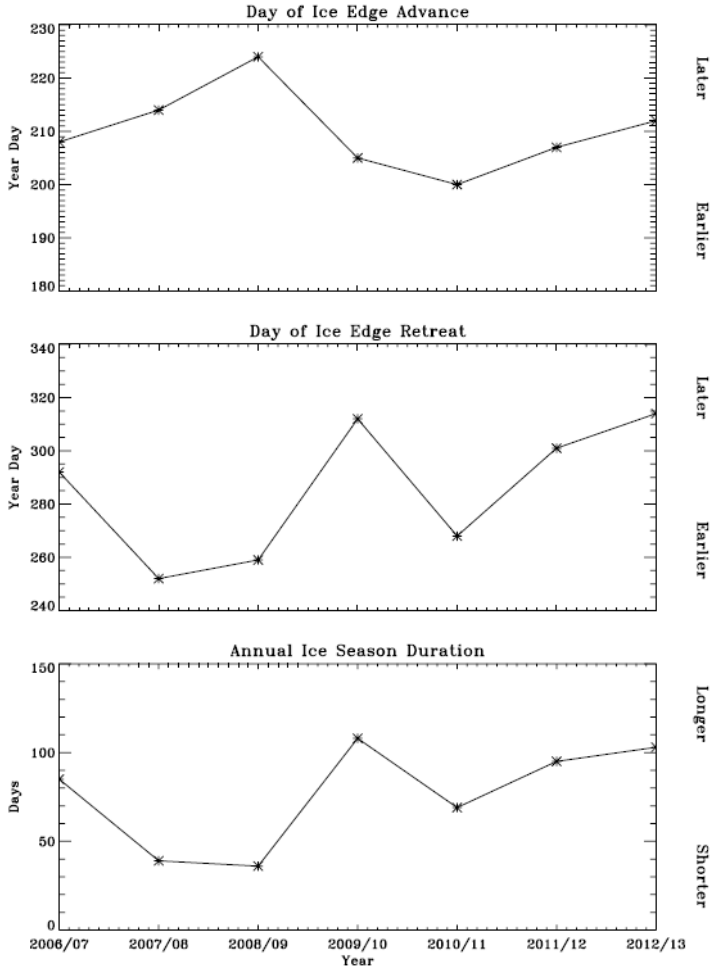

Figure S15: Plots showing day of ice edge advance, retreat and duration, over the sediment trap location and spanning the sediment trap time series.